



CMBEC47/ACCES26 JOINT CONFERENCE

MAY 26-29, 2025
FREDERICTON
NEW BRUNSWICK

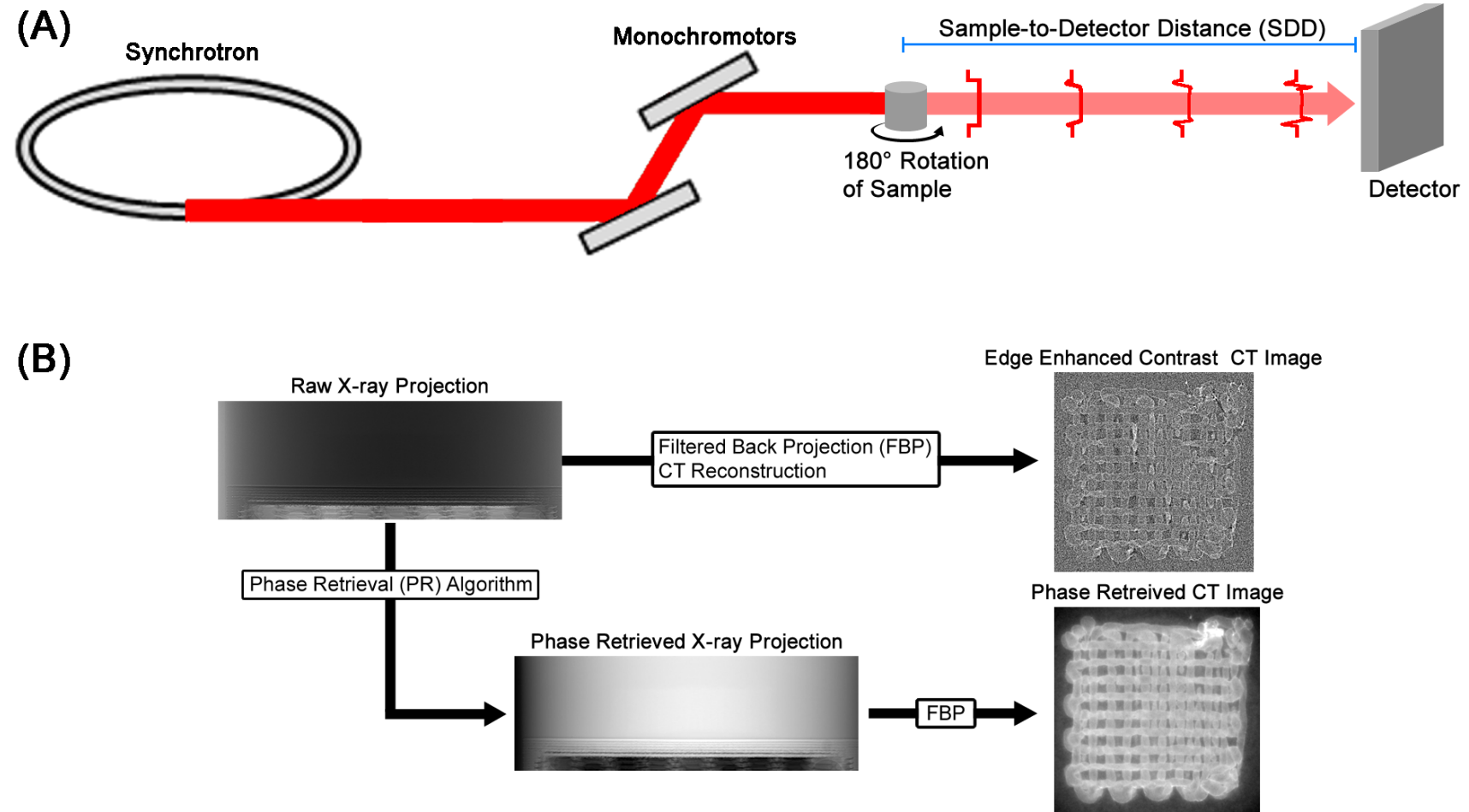
Enhanced Image Processing of Implanted Hydrogel Scaffold Images Using Propagation-Based Imaging Computed Tomography

Xiao Fan Ding, Zahra Khoz, Daniel Chen, Ning Zhu



Introduction

- Synchrotron Radiation Propagation Based Imaging (SR-PBI)
- Phase retrieval (PR)
- Computed tomography (CT)



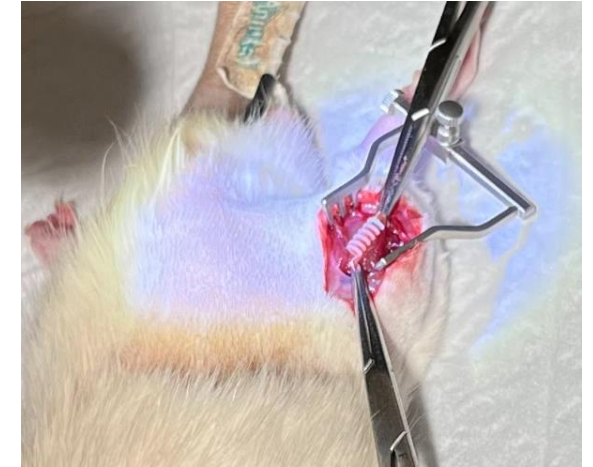
Introduction

- Tissue scaffolds
 - Plays a role in tissue repair
 - Structural support
 - Potentials in personalized medicine
- Visualization techniques
 - Non-destructively evaluate hydrogel scaffolds
 - Especially for longitudinal studies

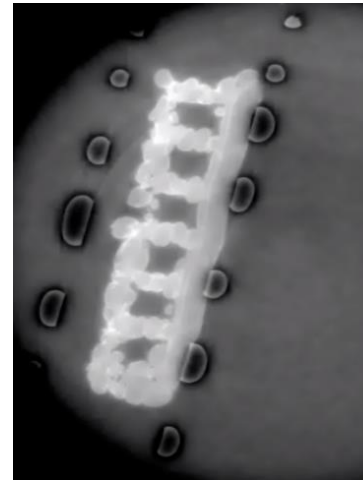
Prepared scaffolds in microcentrifuge tubes



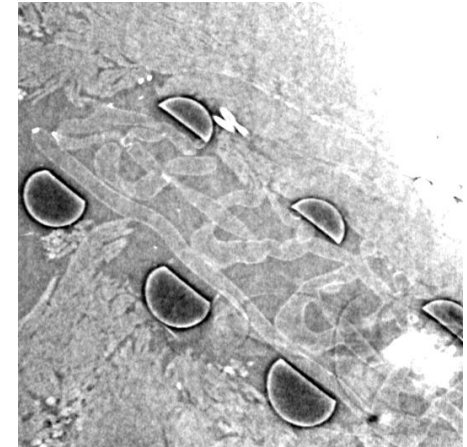
Implantation in at nerve injury site



CT slice of scaffold *In vitro*



CT slice of scaffold *ex vivo*

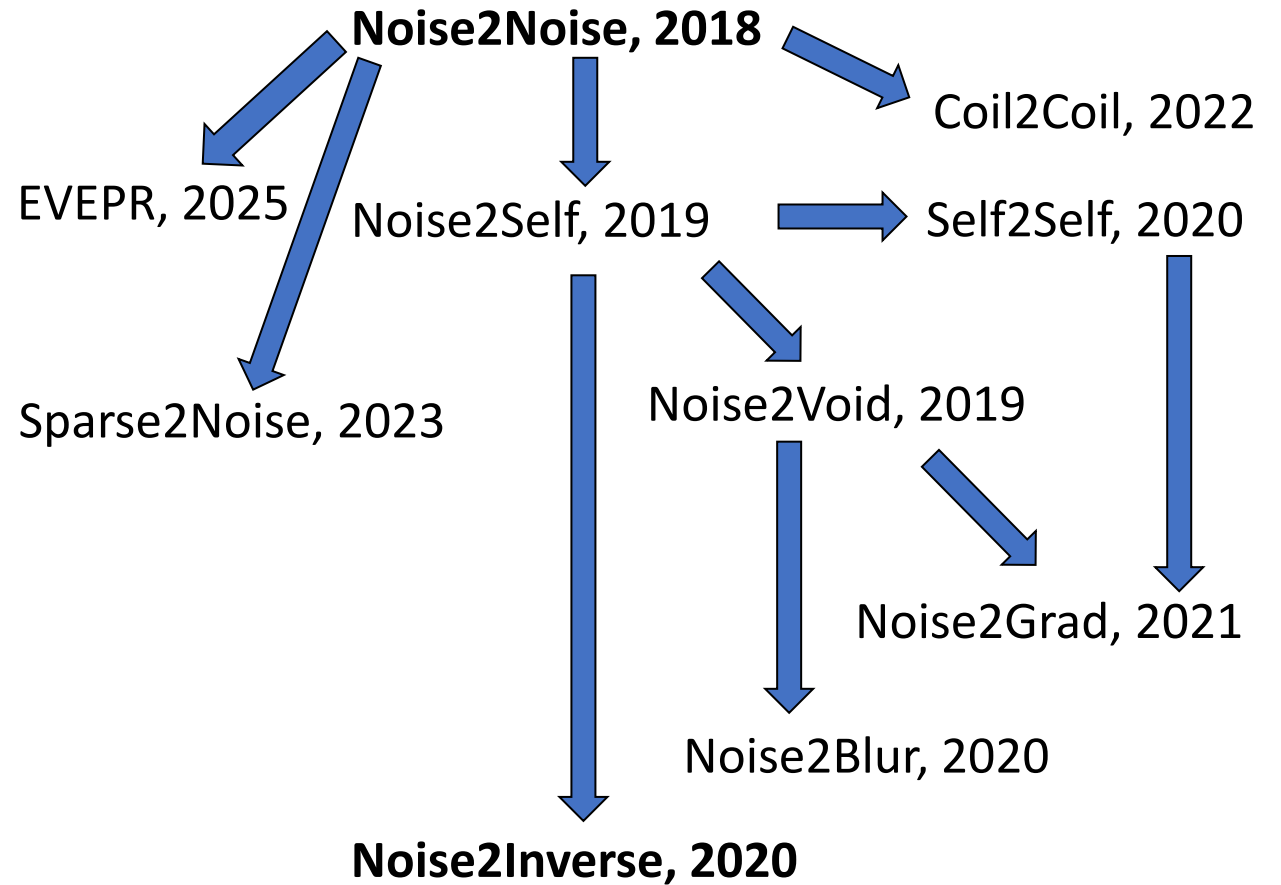


Introduction

Convolution neural networks (CNNs) to reduce image artefacts

$$L(\theta) = \mathbb{E}_{y_1, y_2} [|f_{\theta}(y_1) - y_2|]$$

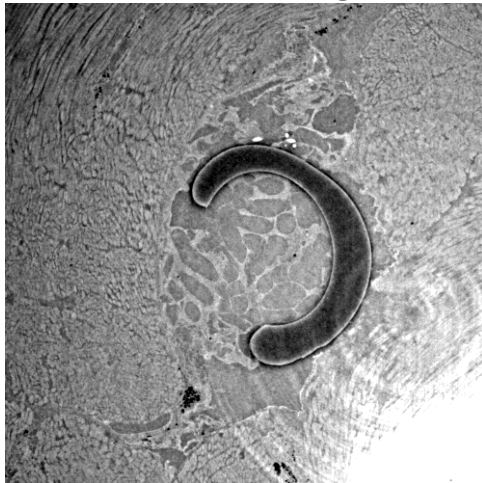
- Neural network, f_{θ}
- Parameterized by θ
- Artefact corrupted images, y_1 and y_2
- Artefact is independent
- Loss function, $L(\theta)$



Introduction

There is a need to improve deep learning denoising performance in *ex vivo* samples acquired with SR-PBI

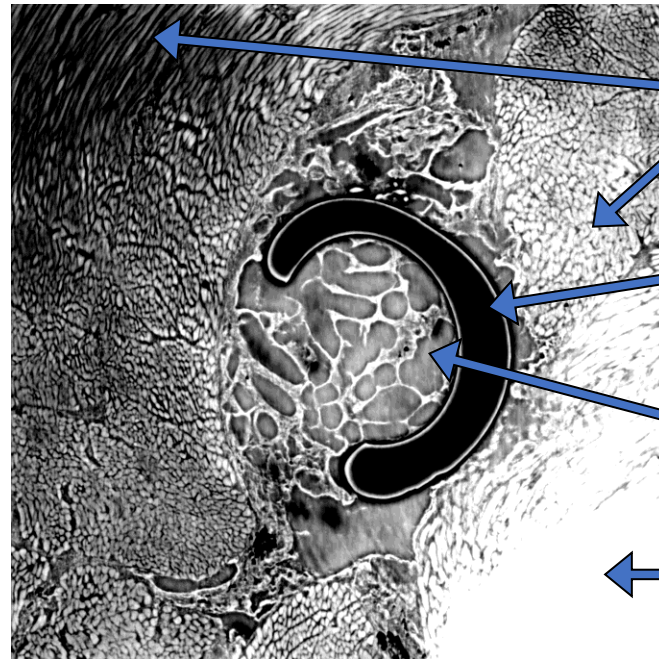
Phase Retrieval Image



Grey Value Histogram



Noise2Noise with bone



Muscle having different contrasts

Achieve consistency in muscle contrast

Stent

Maintain contrast of PCL stent and surrounding tissue

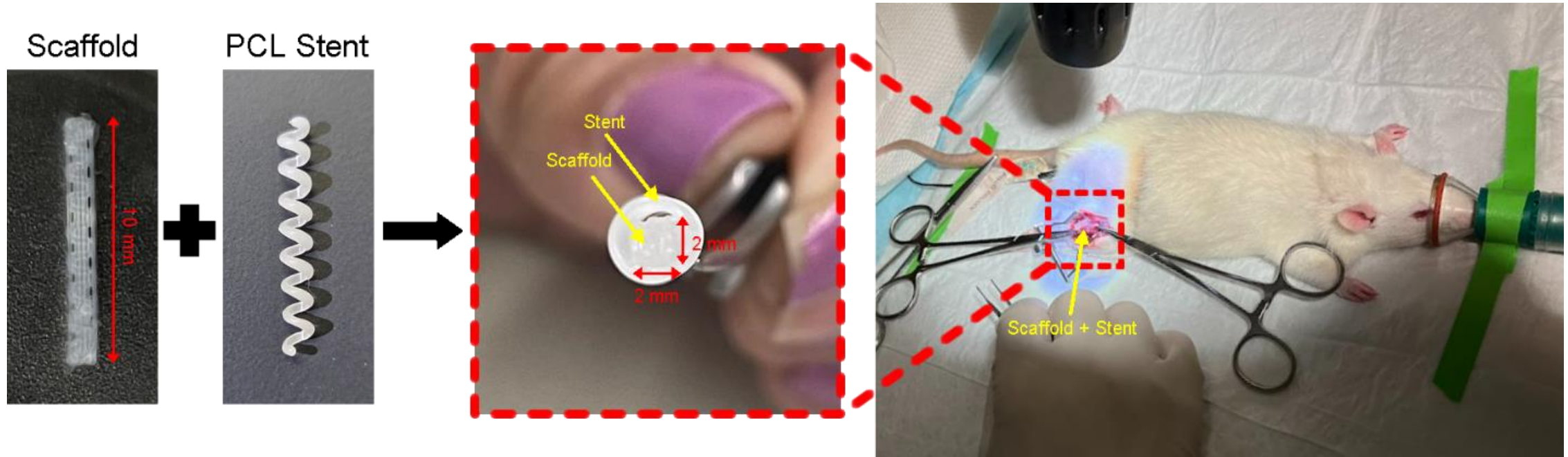
Hydrogel scaffold

Improve contrast between scaffold and surrounding tissue

Presence of bone

Mask the bone with the surrounding tissue

Methods

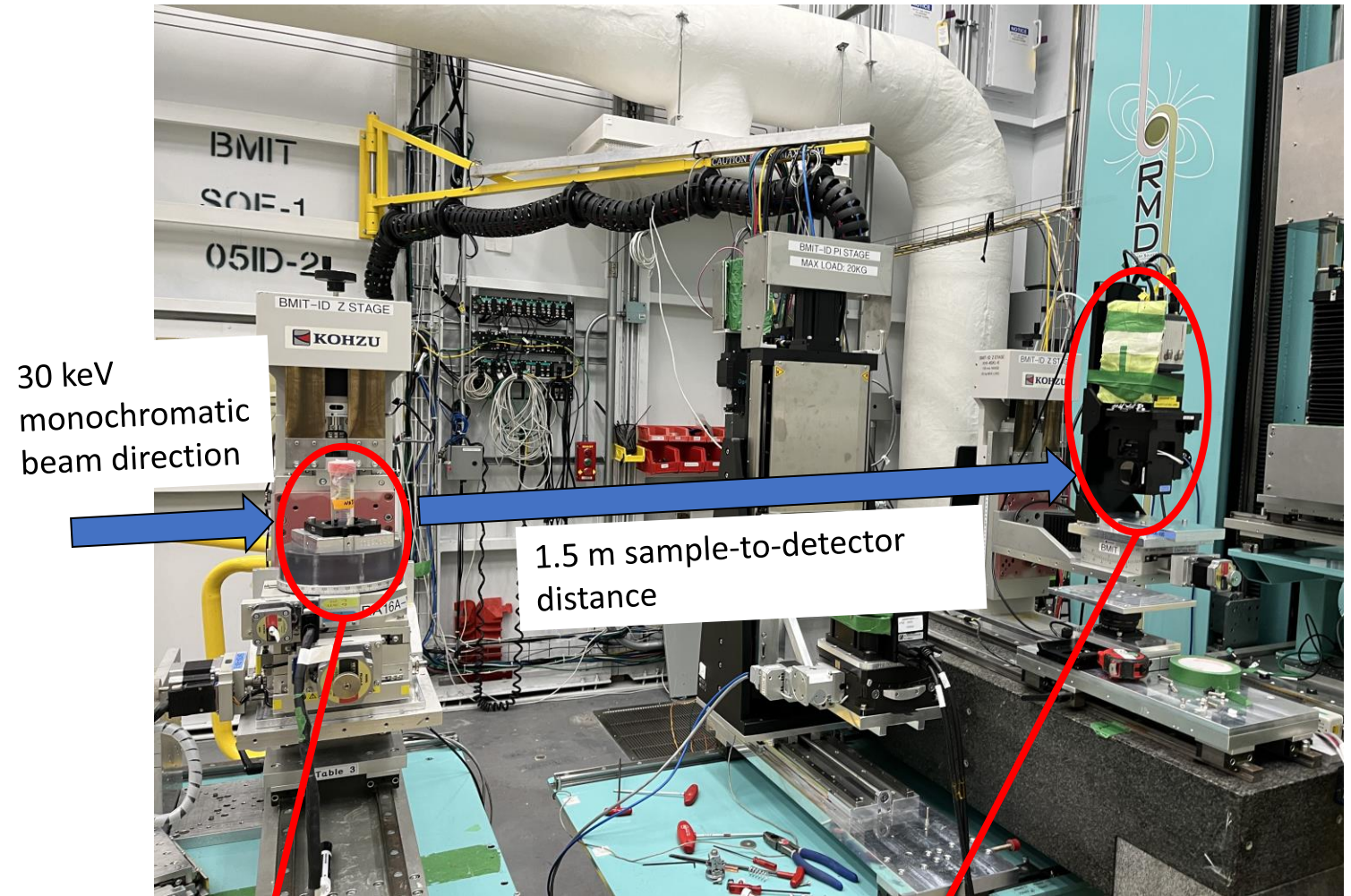


- Hindlimb of Sprague-Dawley rats
- Sciatic nerve was exposed and bisected
- Scaffold inside polycaprolactone (PCL) stent was sutured to the nerve
- Wound closed and rats were allowed to recover before euthanasia

Methods

- Field-of-view of 26.6 by 6.5 mm
- Exposure time of 25 ms
- 3000 projections per dataset
- Acquisition time of 75 s per dataset

Inside the experimental hutch of the BMIT ID beamline at the Canadian Light Source

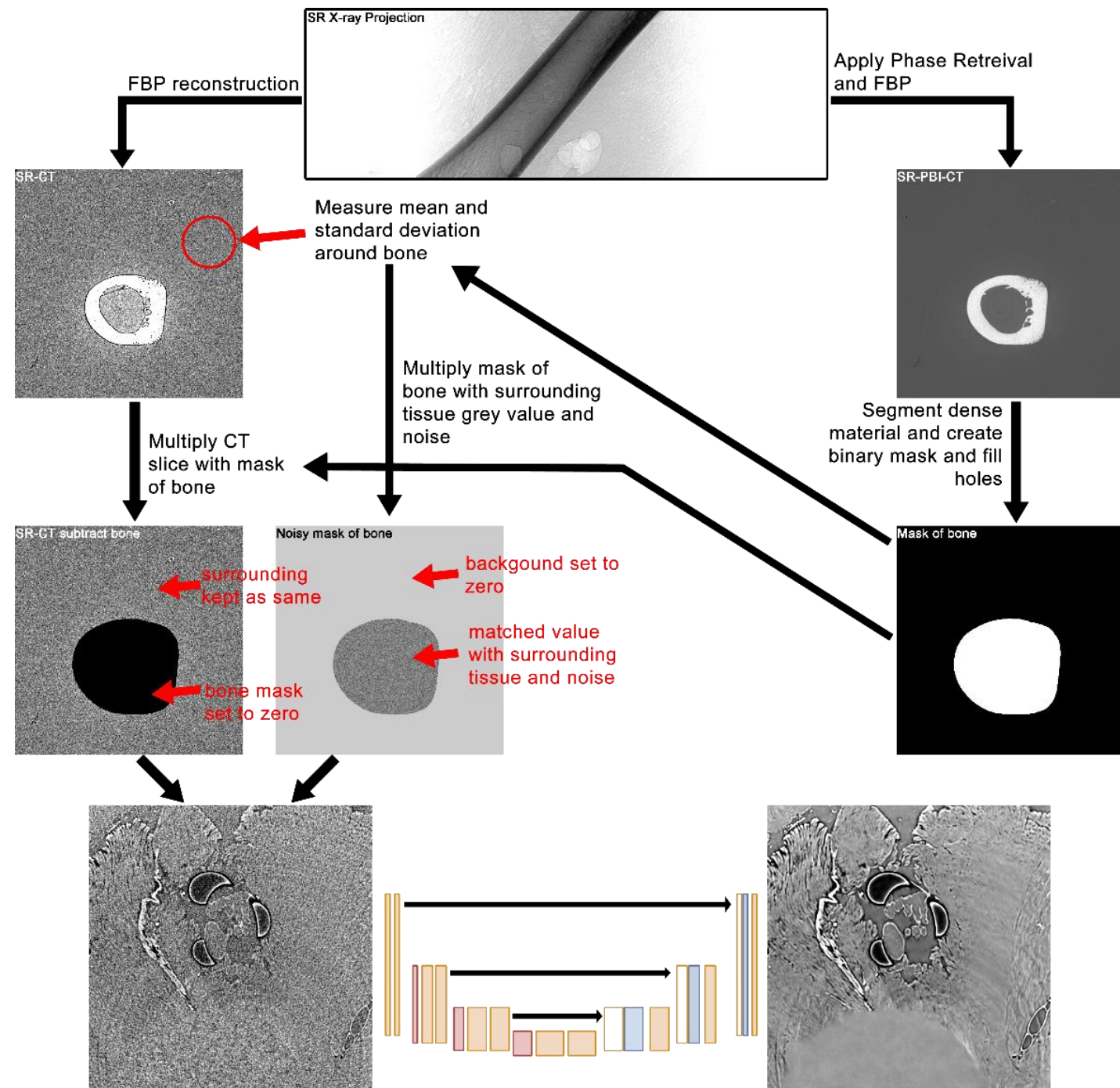


Hind limb sample on top of rotation stage

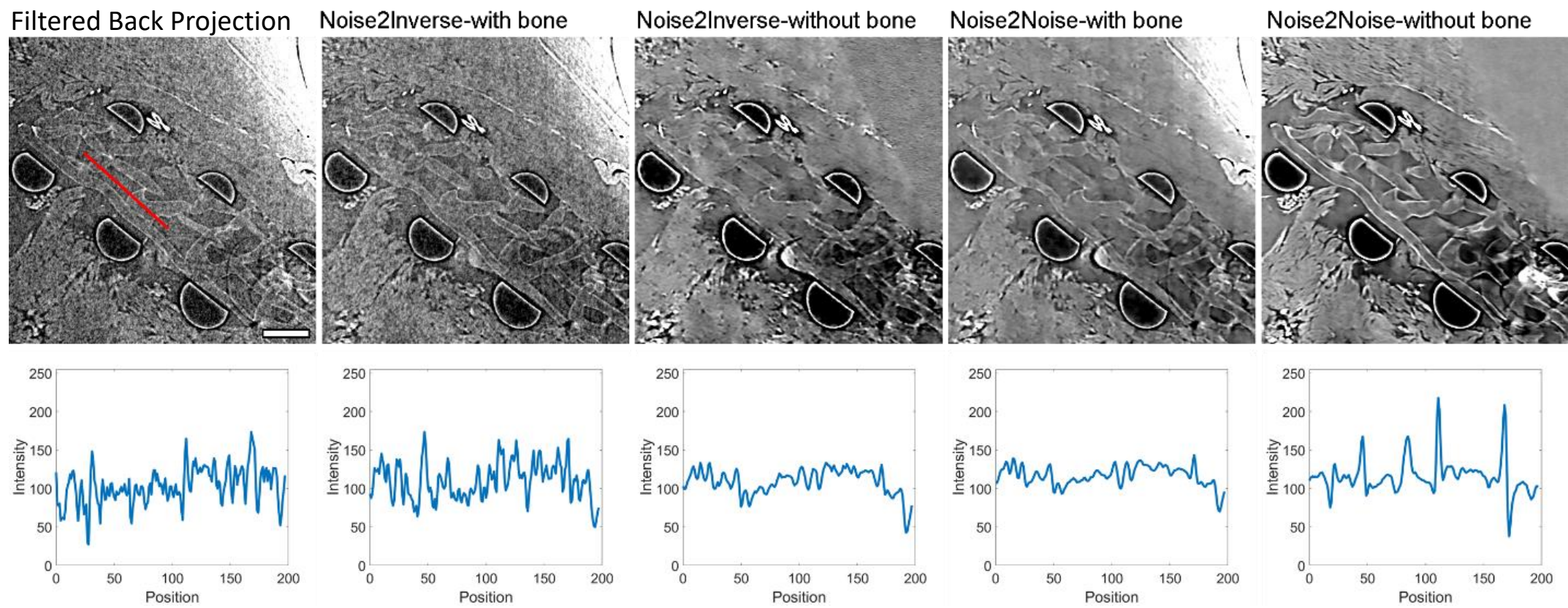
Detector with effective pixel size of 13 μm

Methods

- Raw dataset reconstructed twice:
(1) with phase contrast
(2) without phase contrast
- Bone mask from (1) replace the bone in (2)
- Bone-masked result images used in Noise2Noise and Noise2Inverse



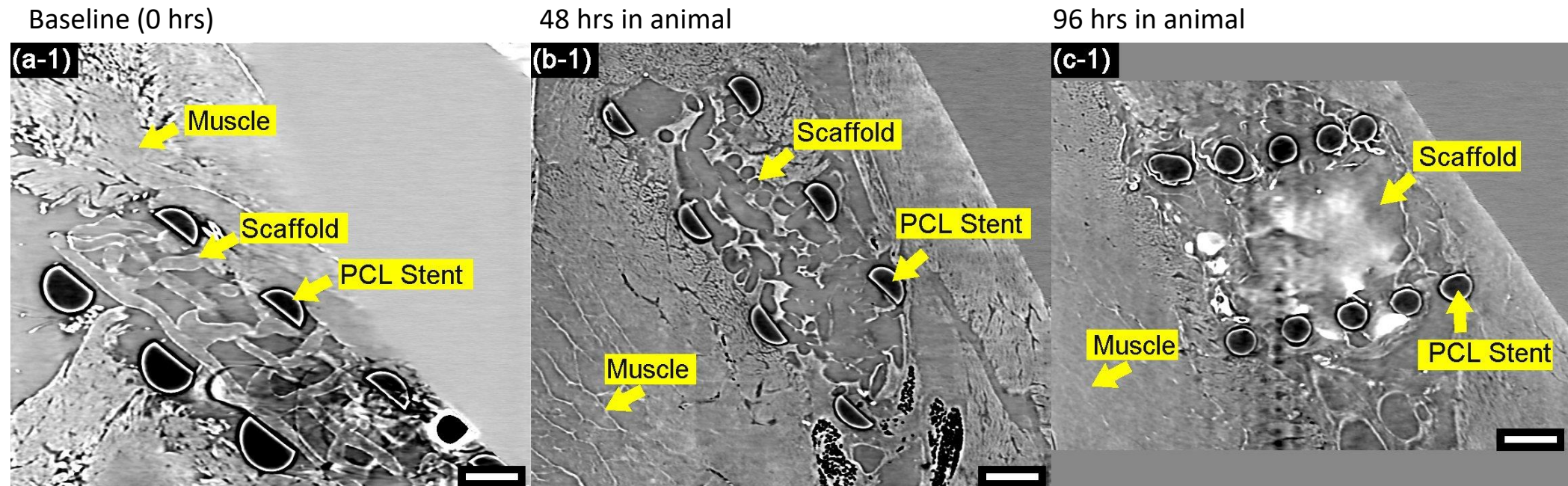
Results



	Filtered Back Projection	Noise2Inverse with bone	Noise2Inves without bone	Noise2Noise with bone	Noise2Noise without bone
SNR	29.21 ± 1.97	42.61 ± 0.25	71.33± 0.58	110.32 ± 31.22	173.06 ± 40.61
CNR	0.54 ± 0.16	0.85 ± 0.19	1.25± 0.29	1.13 ± 0.25	2.19 ± 0.60
PIQE	7.61 ± 0.69	7.96 ± 1.06	7.85 ± 0.78	6.47 ± 0.96	5.44 ± 0.41

Results

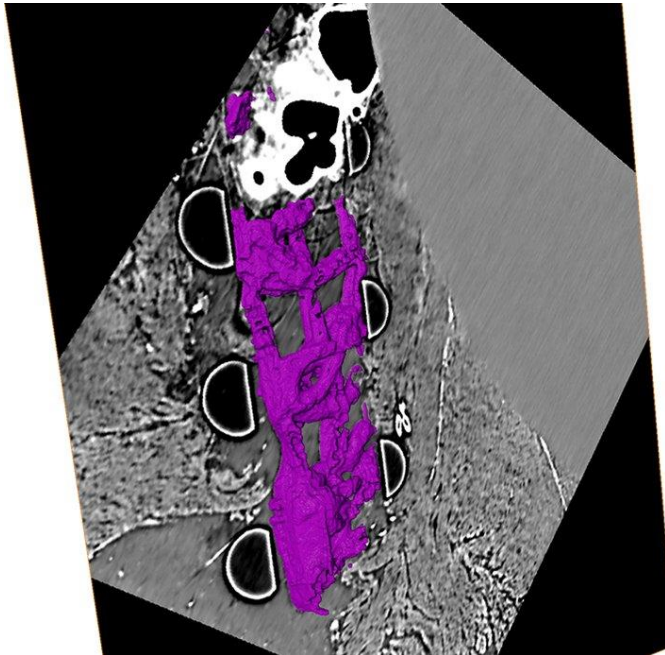
PBI- μ CT scans of rat hindlimb samples containing hydrogel scaffold implant at longitudinal time points:



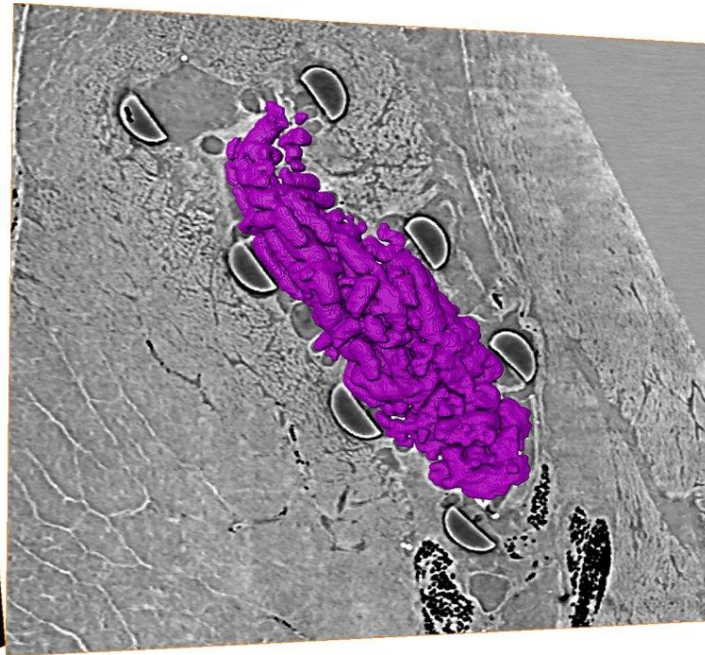
Results

Segmentation and 3D render of stent and scaffold at longitudinal time points:

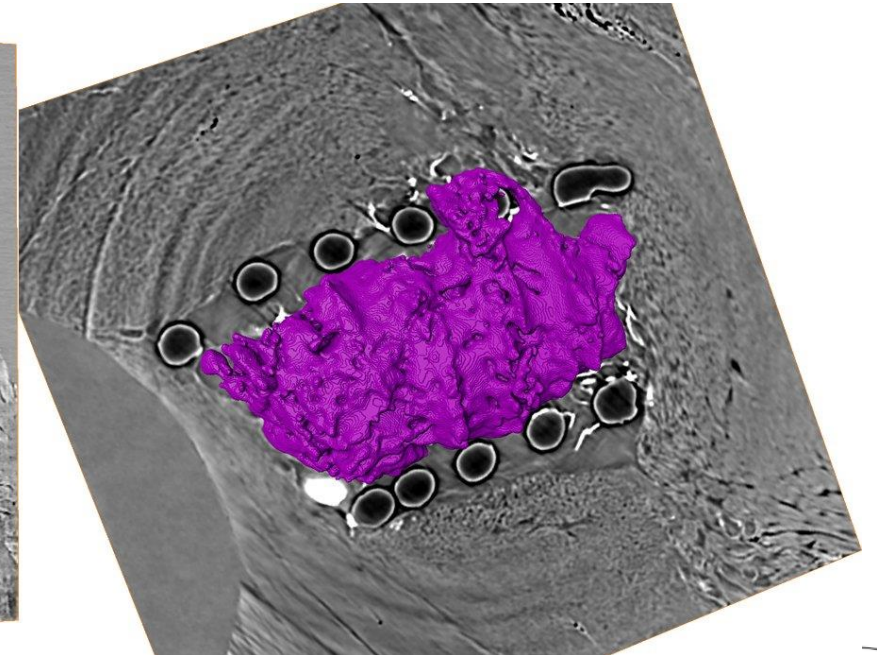
Baseline



2 days in animal

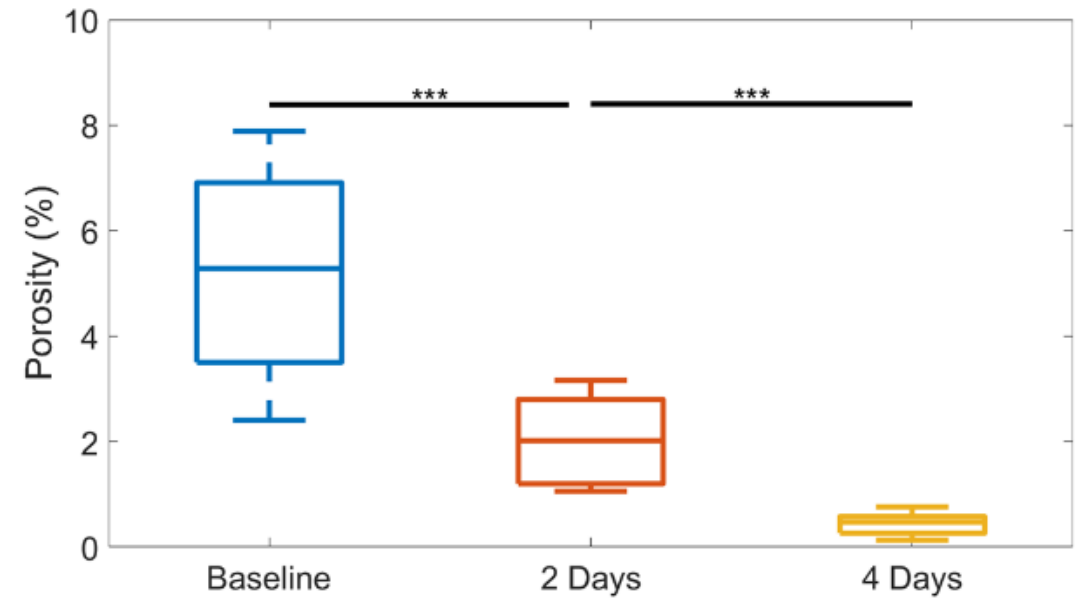
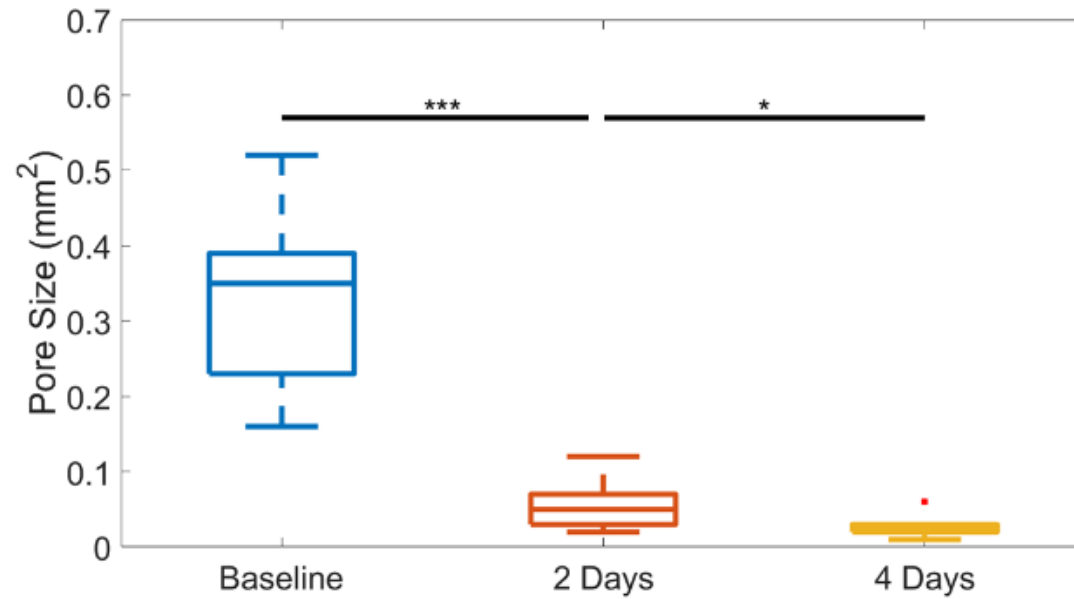


4 days in animal



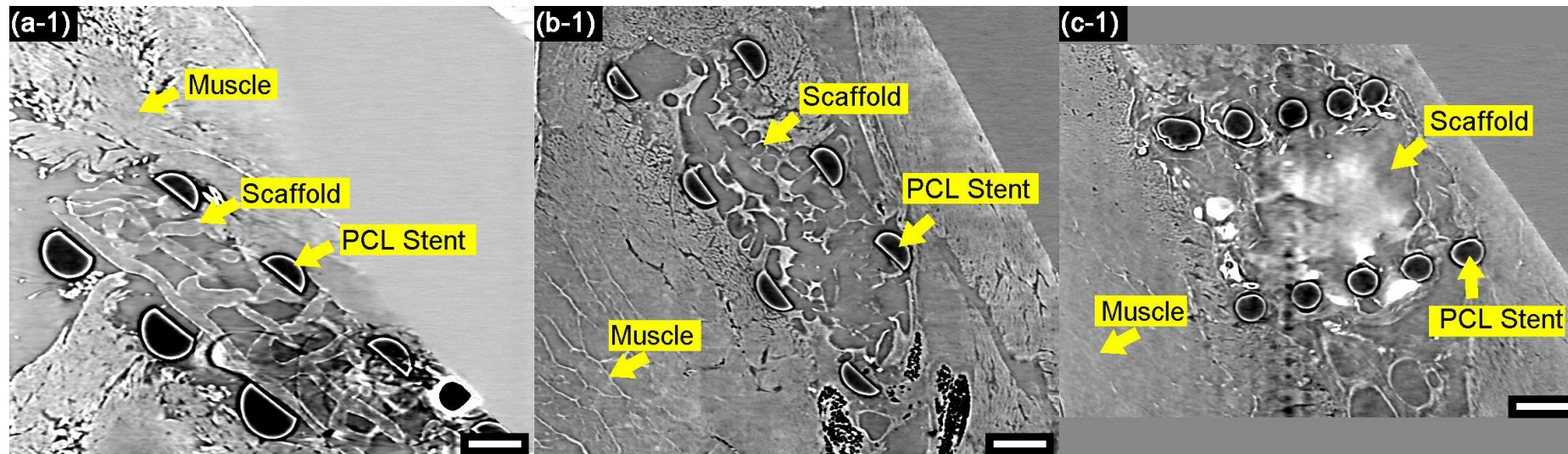
Results

Segmentation and 3D render of stent and scaffold at longitudinal time points:



Conclusion

- Bone masking to enhance the results of deep learning denoising
- Allowed visualization of hydrogel scaffolds *ex vivo*, longitudinal time points
- Next step to study scaffolds in vivo



Acknowledgements



Dr Ning Zhu's Imaging Group

And to the following sources of funding:

